Journal of Ovonic Research Vol. 4, No. 6, December 2008, p. 175 - 180

HYDROTHERMAL PREPARATION, CRYSTAL STRUCTURE OPTICAL AND MAGNETIC PROPERTIES OF $Cd_{1-x}Mn_xS$ NANORODS

M. BOSHTA*, S. A. GAD, A. M. ABO EL-SOUD, M.Z. MOSTAFA[a]
Solid State Physics Dept., National Research Center, El-Bohoos st., 11312 Dokki, Giza, Egypt
[a]*Ceramic, Refractories and Building Materials Dept., National Research Center, El-Bohoos st., 11312 Dokki, Giza, Egypt*

CdMnS semiconductor nanorods were successfully prepared by the hydrothermal reaction of $CdCl_2 \cdot 2.5H_2O$ and $MnCl_2 \cdot 5H_2O$ with $(NH_4)_2S$ in aqueous solution. Energy dispersive X-ray (EDXs) was used to determine the Mn content of these complex nanorods. The samples were characterized by X-ray diffraction (XRD), transmission electron microscopy (TEM), UV–vis. absorption spectra, and compared with the undoped CdS nanorods. The results showed that nanostructured compounds with high aspect ratio were obtained via hydrothermal method. The products showed almost totally rodlike morphology with approximately identical diameters average 14.5nm and maximal lengths up to 80 nm. The magnetic susceptibility measurements were done on $Cd_{1-x}Mn_xS$ samples with different x values.

(Received December 8, 2008; accepted December 12, 2008)

1. Introduction

Recently much progress has been made for preparing and characterizing dilute magnetic semiconductors with nanocrystal materials of wide variety [1-3]. Dilute magnetic semiconductors (DMS) are ternary alloys in which cations of semiconductor matrix are randomly substituted by magnetic ions that exhibit unique physical and chemical properties due to confinement effect [4,5]. Mn-based compounds have been extensively investigated as typical diluted magnetic semiconductors because of their wide direct band gaps and outstanding magneto-optical properties [6-8].

The presence of localized magnetic ions such as Mn^{2+} in semiconductor alloys leads to exchange interactions between s-p band electrons and manganese d-electrons with altered band gap. So it is important to investigate the optical properties of DMS since their deep or shallow trap states contain useful information about the quantum size effect in the electron or hole bound to the trap center. Optical properties attributed to quantum size effect have been studied before by several groups [8,11]. The Mn-based DMS can be grown over a wider composition range than Fe- and Co- based DMS [(9).] Because of tunable band gaps, lattice parameters of the Mn-based alloys are excellent candidates for fabrication* of quantum wells and superlattices [7,10]. Numerous reports have been devoted to either semiconducting or magnetic properties of only selenides and tellurides. However, studies on sulphide are very few.

In this paper the preparation of $Cd_{1-x}Mn_xS$ DMS nanorods by hydrothermal method was tried. Then the morphology and composition of the prepared samples with different manganese content were characterized by XRD patterns. Transmission Electron Microscopy (TEM) as well as Energy Dispersive X-ray spectrometer (EDXs), optical properties and magnetic properties were studied and reported.

*Corresponding author: boshta@hotmail.com

2. Experimental procedure

$Cd_{1-x}Mn_xS$ nanorods were hydrothermally prepared. All chemicals used in the present work were analytical-grade without any further purification. The steps involved in this hydrothermal process can be described as follows.

1.14 g of $CdCl_2$.2.5ml H_2O and various amounts of $MnCl_2.5H_2O$ verify the concentration of Mn with x= 0.05, 0.10, 0.15, and 0.20 were placed into the 50ml Teflon-lined stainless steel autoclave which has been filled with 30g of distilled water and 20g of ethylendiamine. In the next step, 0.4g of $(NH_4)_2S$ were injected dropwise into the used autoclave with a syringe. A clear yellow solution was obtained due to the reaction of Cd^{2+}, Mn^{2+} and S^{2-}. The autoclave was sealed carefully and put into an oven maintained at 180^{o}C for 48 hours, then cooled down to room temperature gradually. The precipitates were separated from the aqueous solution and washed with absolute ethanol and then distilled water repeatedly. The final products were dried in a vacuum at 60^{o}C for four hours and were collected for characterization.

The elemental composition of the synthesized materials in powder form were determined by using the energy dispersive X-ray spectrometer (EDXs) unit that interfaced to Scanning Electron Microscope (SEM)(Philips-XL) operating at an accelerating voltage of 30 KV. The relative error of determining the indicated elements did not exceed 5%.

The X-ray diffraction patterns were obtained using computer controlled X-ray diffractometer (formally made by Diano cooperation).

Samples for TEM were prepared by putting a few drops of absolute ethanol solution of ultrasonically dispersed products on a copper grid. TEM micrographs and corresponding diffraction patterns were taken on Jeol TEM-1230 Electron Microscope at high tension of 120 KV.

Optical absorption was recorded on a spectrophotometer type (Jasco V-570) by scanning the absolute ethanol solution in 1cm quartz cell as a reference for the samples that were dispersed on the same amount of absolute ethanol. The wavelength range was scanned from 200nm to 700 nm.

Magnetization behavior of $Cd_{1-x}Mn_xS$ system for x = 0.05, 0.01, 0.15 and 0.2 were studied at room temperature in the magnetic field up to 100 kOe using a vibrating sample magnetometer model 960001-VSM.

3. Results and discussion

3.1. Composition analysis

The atomic percentage and/or weight percentage of elemental composition of the prepared materials are computed from analysis of energy dispersive X-ray spectrometry (EDXs). The composition analysis of the four compounds of $Cd_{1-x}Mn_xS$ with indicated x confirmed the presence of Cd, Mn and S elements. From the obtained results, it is revealed that all the prepared samples are nearly stoichometric with an error not exceed 5%.

3.2. XRD Characterization

The X-ray diffraction patterns of the synthesized materials are shown in Fig. 1.

Although, the general form has the same features, the peak positions shift slightly on passing from one composition to the other. All the patterns can be distinctly assigned to the hexagonal Cadmium Sulphide phase with six main diffraction peaks which are corresponding to (002), (100), (101), (110), (103) and (112) planes. It is also clear from this figure that in all the XRD patterns, the broadening of the diffraction peaks indicate the nanostructure nature of the samples which agree well with the work done by Qingsheny et al.[(11)].

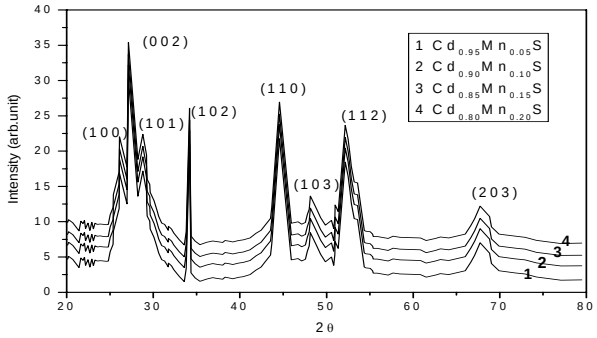

Fig. 1. XRD patterns for $Cd_{1-x}Mn_xS$ prepared samples with different x-values.

3.3. Morphology analysis:

TEM was used to measure the particle size of the prepared nanostructure materials. Fig. 2. shows TEM images of the four tested compositions. It is clear from this figure that $Cd_{1-x}Mn_xS$ are almost all rod-like and the yield of the nanorod is about >85%. A general view of TEM images of the prepared compositions at low magnification in Fig.(3) demonstrates that the diameter of the nanorods are around (11 nm-14.5 nm) and the lengths vary from 45 nm-80 nm.

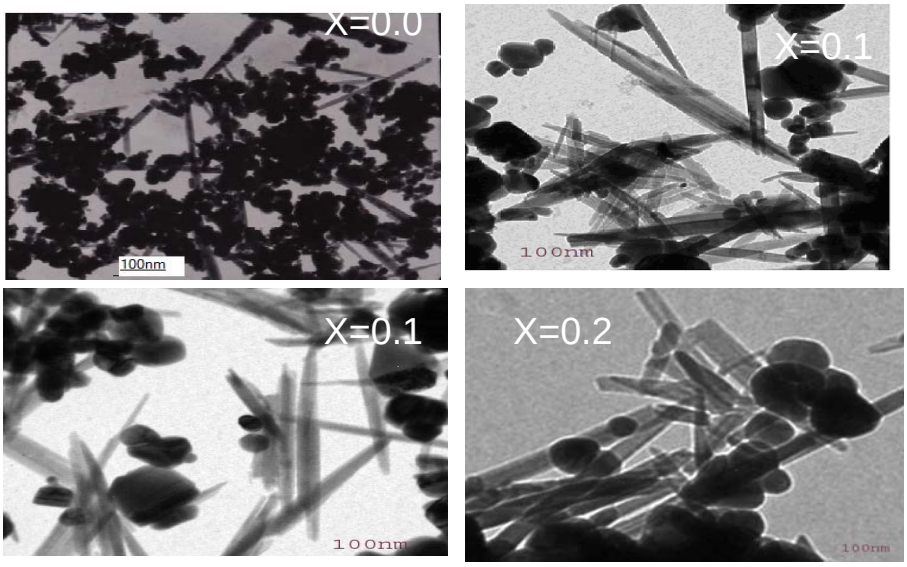

Fig. 2. TEM images for $Cd_{1-x}Mn_xS$ samples with different x-values.

3.4. Optical analysis

The optical absorption spectra of $Cd_{1-x}Mn_xS$ at room temperature are shown in Fig 3. It is clear that all the absorption band edges shift a little to shorter wavelength with increasing the Manganese content which agree well with the published work of Wang et al.,[12,13] while Levy et al. observed a nonlinear increase in the band edge of $Cd_{1-x}Mn_xS$ nanoparticles with increasing the amount of Mn[14]. But Reddly et al.,[15] found for prepared thin films of these compositions that the optical band gap decreases directly with increasing of the Mn concentration, and explained this behaviors on the basis of the chemical bonding between atoms. The unsaturated bonds that might be present in the film at low Mn concentrations are responsible for the formation of some defects

which produce localized state in the band structure and therefore reducing the optical band gap. For colloidal nanoparticles of CdS an absorption threshold can be seen at 2.62eV corresponding to the lowest 1s-1s transition. Whereas for colloidal nanoparticles of CdMnS an absorption threshold can be seen at 2.83 eV [16].

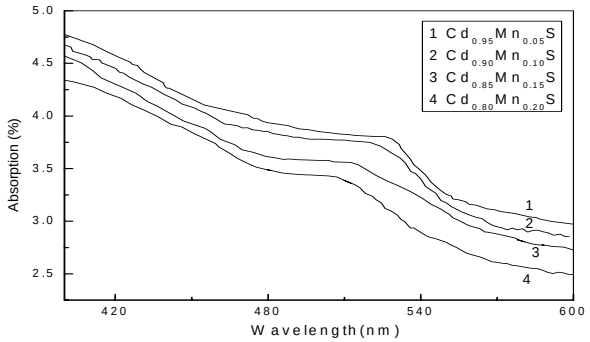

Fig.3. Absorbance of $Cd_{1-x}Mn_xS$ samples with different x-values versus the wavelength.

3.5. Magnetic Properties:

3.5.1. Hysteresis loop and susceptibility:

The magnetic behavior of $Cd_{1-x}Mn_xS$ powder has been studied as a function of Mn concentration. Fig 4. shows the magnetic hysteresis loop of $Cd_{1-x}Mn_xS$ powder at room temperature. It is clear from this figure that the hysteresis loop is symmetric with respect to zero fields.

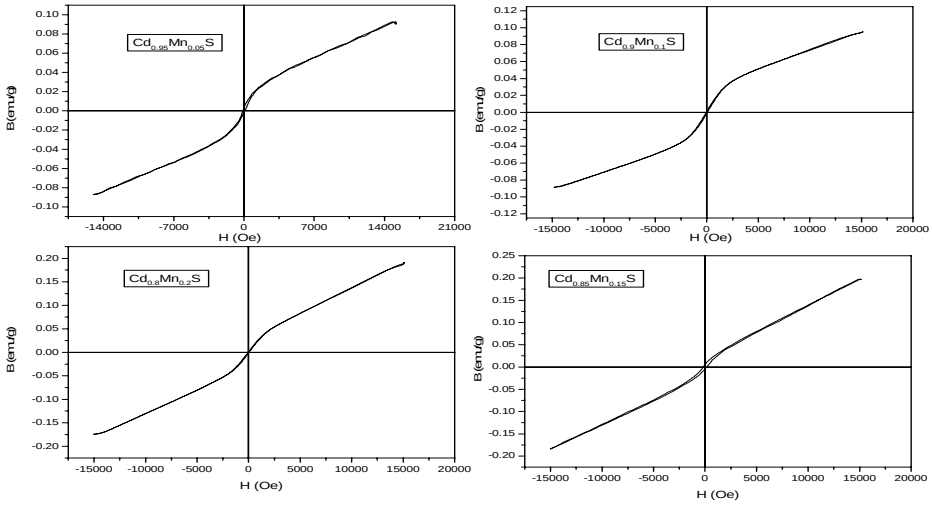

Fig. 4. Hysteresis loop of $Cd_{1-x}Mn_xS$ samples with different x values at room temperature.

The magnetic saturation induction B_s increases with increasing the Mn concentration. Also, the coercive force H_c increases with increasing the Mn concentration for x= 0.05, 0.10 and 0.15 and then decreases for x=0.20. The increase of H_c with Mn concentration is due to the ferromagnetic behavior of CdMnS samples.

The magnetic susceptibility studies were carried out at room temperature and magnetic field 10KOe using vibrating sample magnetometer. Fig.5. shows the magnetic susceptibility as a function of Mn concentration. It is clear from the figure that the susceptibility varies nonlinearly with increasing of the Mn concentration. Veer Brahnam et al., [17], found the same behavior in Zn_{1-}

$_xMn_xTe$ at room temperature and the slope of the susceptibility at lower concentration is more compared with the slope at higher concentration. This behavior may be understood in this material by the fact that each Mn^{+2} ion has a total spin s =5/2 originating from the half-field "3d" shells. Mn^{+2} spins are coupled by short-range antiferromagnetic interaction [8].

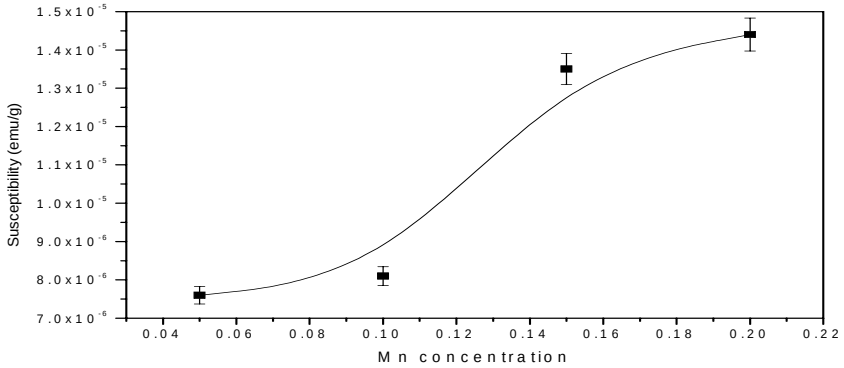

Fig. 5. The magnetic susceptibility of $Cd_{1-x}Mn_xS$ samples versus the Mn concentration

Nonlinear variation of susceptibility with respect to the composition (x) may be explained as follows. At lower concentration of Mn, the "sp" electrons with spin opposite to the spin of the atom in ZnTe lattice interact with spin of Mn atom, which causes a decrease in susceptibility. At higher concentrations of Mn, the d-d exchange interaction between Mn atoms dominates over the sp-d exchange interaction resulting in an abrupt increase in susceptibility [(18)].

4. Conclusions

In summary, one can demonstrate that the hydrothermal process is a good technique for the synthesis of DMS nanorods. The Mn content is determined and all our results are consistent with each other very well. EDX spectra confirmed that the composition is Mn. The nanorods prepared as such have high productive rate and are rod-like with a diameter of about 14.5 nm. From repeated TEM examinations and powder XRD patterns of $Cd_{1-x}Mn_xS$ are indexed as the hexagonal phase just as CdS. When Cd^{2+} is partly substituted by Mn^{2+} ions, the absorption band edge of $Cd_{1-x}Mn_xS$ moves to shorter wavelength relative to CdS. The magnetic susceptibility of $Cd_{1-x}Mn_xS$ samples varies nonlinearly with increasing of the Mn concentration.

References

[1] Mann S., G .A. Ozin, Nature **382**, 313 (1996).
[2] Wang J., M. S. Gudiksen, X. Duan, Y. Cui, C. M. Lieber, Science **293**,1455 (2001).
[3] Bachtold A., P. Hadley, T. Nakanishi, C. Dekker, Science **294**,1317 (2001).
[4] Brus L. E., Applied Physics **A53**,465 (1991).
[5] Weller H., Angew. Chem. **105**,43 (1993).
[6] Alivisator A. P., Science **271**,933 (1996).
[7] Jonker B. T., X. Liu, W. C. Chou, A. Petrou, J. Warnock, J. J. Krebs, G. A. Prinz, J. Appl. Phys. **69**, 6098(1991).
[8] Murase N., R. Jagannathan, Y. Kanematw, M. Walanabe, A. Kurita, K. H. Irata, T. Yazawa, T. Kushida, J. Phys. Chem. B **103**,754 (1999).
[9] Mukesh J. (Ed) “Dilute magnetic semiconductors”, World scientific, Singapore (1991).
[10] Chou W. C., A. Petrou, J. Warnock, B. T Jonker, Phys. Rev. Lett. **67**,3820 (1991).
[11] Bhargava R. N. D. Gallagher, X. Hong, A. Nurmikko, Phys. Rev. Lett.**72**(3), 416-419 (1994).

[12] Wang Q. S., Z. D. Xu, Q. L. Nie, L. H. Yue, W. X. Chen, Y. F. Zheng, Solid Stat communications **130**,607-611(2004).
[13] Wang Qingsheng, Zhude Xu, Linhai Yue, Weixiang Chen, *Optical* Materials 27,453-458 (2004).
[14] Levy L., N. Feltin, D. Intgrt, M. P. Pileni, J. Phys. Chem. **B101**, 9153 (1997).
[15] Streekantha Reddy D., D. Raja Reddy, B. K. Reddy, N. Koteeswara Reddy, K. R. Gunasekhar, P. Sradhara Reddy, Optical Materials xxx (2007) xxx
[16] Savchuk A. I., V. I. Fediv, A. G. Voloshchuk, T. A. Savchuk, Yu Yu Bacherikov, A. Perrone, Material Science and Engineering **C26**,809-812 (2006).
[17] Veer Brahnam K., D. Raja Reddy and B. K. Reddy, Acta part A; Molecular and Biomolecular Spectroscope **60**,741-745 (2004).
[18] Spalek J., A. Lewicki, Z. Taynawski, J. K. Furdyna, R. R. Galazka and Z. Obuszko, Phys. Rev. B **33**, 3407 (1985).